

Envelope Equations for Three-Dimensional Gravity and Flexural-Gravity Waves Based on a Hamiltonian Approach

Philippe Guyenne

Dedicated to Walter Craig on the occasion of his 60th birthday, with admiration and gratitude.

Abstract A Hamiltonian formulation for three-dimensional nonlinear flexural-gravity waves propagating at the surface of an ideal fluid covered by a thin ice sheet is presented. This is accomplished by introducing the Dirichlet–Neumann operator which reduces the original Laplace problem to a lower-dimensional system involving quantities evaluated at the fluid-ice interface alone. The ice-sheet model is based on the special Cosserat theory for hyperelastic shells, which yields a conservative and nonlinear expression for the bending force. By applying a Hamiltonian perturbation approach suitable for such a formulation, weakly nonlinear envelope equations for small-amplitude waves are derived. The various steps of this formal derivation are discussed including the modulational Ansatz, canonical transformations and expansions of the Hamiltonian. In particular, the contributions from higher harmonics are examined. Both cases of finite and infinite depth are considered, and comparison with direct numerical simulations is shown.

1 Introduction

Modulation theory is a well-established method in applied mathematics to study the long-time evolution and stability of oscillatory solutions to partial differential equations. Typical equations to which the theory is applied are nonlinear dispersive evolution equations describing wave phenomena that arise in physical applications. Examples include ocean waves as well as waves in optics and plasmas. The usual modulational Ansatz is to anticipate a weakly nonlinear monochromatic form for solutions, and to derive equations describing the evolution of their envelope. In two space dimensions (i.e. one-dimensional wave propagation), the first nontrivial terms typically yield the nonlinear Schrödinger (NLS) equation [38], while the

P. Guyenne (✉)

Department of Mathematical Sciences, University of Delaware, Newark, DE 19716, USA
e-mail: guyenne@udel.edu

Benney–Roskes–Davey–Stewartson (DS) system arises in three dimensions. The rigorous justification of these models is a challenging mathematical problem [13, 15, 27, 35] and recent breakthroughs have been made in the two-dimensional case [16, 40].

Of particular interest here are hydroelasticity problems dealing with the interaction between moving fluids and deformable bodies. Such problems not only entail considerable mathematical challenges but also have many engineering applications [26]. An important area of application is that devoted to hydroelastic (or flexural-gravity) waves in polar regions where water is frozen in winter and the resulting ice cover is transformed e.g. into roads and aircraft runways, and where air-cushioned vehicles are used to break the ice. A major difficulty in this problem has to do with modeling the ice deformations subject to water wave motions [36]. Theories based on potential flow and on the assumption that the ice cover may be viewed as a thin elastic sheet have been widely used [37]. In this context, most studies have considered linear approximations of the problem, which are valid only for small-amplitude water waves and ice deflections.

Intense waves-in-ice events, however, have also been reported and their analysis indicates that linear theories are not adequate for describing large-amplitude ice deflections [28]. In the last few decades, a number of numerical and theoretical investigations have used nonlinear models based on Kirchhoff–Love plate theory to analyze two-dimensional hydroelastic waves in ice sheets. For example, Forbes [17] computed finite-amplitude periodic waves by using a Fourier series expansion technique. Părău and Dias [32] derived a forced NLS equation for the envelope of ice-sheet deflections due to a moving load, and showed that solitary waves of elevation and depression exist for certain ranges of water depth. Bonnefoy et al. [4] examined numerically the same nonlinear problem of moving load on ice, through a high-order spectral approach, and found a good agreement with theoretical predictions of Părău and Dias [32]. Hegarty and Squire [25] simulated the interaction of large-amplitude water waves with a compliant floating raft such as a sea-ice floe, by expanding the solution as a series and evaluating it with a boundary integral method. Vanden-Broeck and Părău [42] computed periodic waves and generalized solitary waves on deep water by using a series truncation method. Milewski et al. [29] derived a defocusing NLS equation which indicates that small-amplitude solitary wavepackets do not exist on deep water. Their direct numerical simulations, based on conformal mapping, reveal however stable large-amplitude solitary waves of depression. Another nonlinear formulation is Plotnikov and Toland’s adaptation of the special Cosserat theory for hyperelastic shells [34], which explicitly conserves elastic potential energy unlike Kirchhoff–Love theory. Guyenne and Părău [21–23] took advantage of this conservative property to write a Hamiltonian form of the flexural-gravity wave problem in arbitrary depth. Their asymptotic and numerical results were found to be consistent with those of Părău and Dias [32] and Milewski et al. [29]. In the long-wave regime, Xia and Shen [43]

established a 5th-order Korteweg–de Vries equation for the nonlinear interaction of ice cover with shallow-water waves. However, a linear Euler–Bernoulli model was adopted for the ice cover.

There have been fewer studies of the three-dimensional nonlinear problem which has drawn serious attention only recently. In a weakly nonlinear setting similar to Xia and Shen's [43], Hărăguș-Courcelle and Ilichev [24] derived a Kadomtsev–Petviashvili equation for weakly three-dimensional flexural-gravity waves on shallow water, while Alam [3] obtained a DS system that admits fully localized dromion solutions. Părău and Vanden-Broeck [33] computed solitary lumps due to a steadily moving pressure, by solving the full nonlinear equations for the fluid combined with a linear Euler–Bernoulli ice sheet. More recently, Milewski and Wang [30] proposed a DS model based on the nonlinear formulation of Plotnikov and Toland [34]. These previous authors [3, 24, 30] used the standard method of multiple scales to derive their models.

In the present paper, we extend the theoretical results of Guyenne and Părău [21–23] to the three-dimensional case. After establishing the Hamiltonian formulation of the problem, we apply the perturbation approach of Craig et al. [8, 10] to deriving envelope equations for weakly nonlinear flexural-gravity waves in the modulational regime. This is accomplished by introducing and expanding the Dirichlet–Neumann operator (DNO) which allows us to reduce the original Laplace problem to a lower-dimensional system involving quantities evaluated at the fluid-ice interface alone. A new aspect of our contribution to this approach is the inclusion of higher harmonics in the modulational Ansatz and the associated canonical transformations. Both cases of finite and infinite depth are considered. The resulting NLS and DS equations resemble existing ones in their general forms, but details such as their numerical coefficients and the relation of their dependent variables to the original physical variables are different. An analysis of these models in the two-dimensional case is performed and their predictions are compared with direct numerical simulations of the full equations. We also explore the possibility of including the exact linear dispersion relation in these approximations to improve their dispersive properties.

The remainder of the paper is organized as follows. Section 2 presents the mathematical formulation of the three-dimensional hydroelastic problem in arbitrary depth. The DNO is introduced and the Hamiltonian equations of motion are established. From this Hamiltonian formulation, weakly nonlinear envelope equations for two- and three-dimensional small-amplitude waves are derived at a formal level in Sect. 3. The various steps of the perturbation method are discussed including the modulational Ansatz, canonical transformation and expansions of the Hamiltonian. Furthermore, comparison with two-dimensional direct numerical simulations is shown and models incorporating the exact linear dispersion relation are also examined. Finally, concluding remarks are given in Sect. 4.

2 Mathematical Formulation

2.1 Equations of Motion

We consider a three-dimensional fluid (e.g. water) of uniform depth h beneath a continuous thin elastic plate (e.g. a floating ice sheet). The fluid is assumed to be incompressible and inviscid, and the flow to be irrotational. The ice sheet is modeled by using the special Cosserat theory of hyperelastic shells in Cartesian coordinates (x, y, z) [34], with the horizontal (x, y) -plane being the bottom of the ice sheet at rest and the z -axis directed vertically upwards (see Fig. 1). The vertical deformation of the ice is denoted by $z = \eta(x, y, t)$. The fluid velocity potential $\Phi(x, y, z, t)$ satisfies the Laplace equation

$$\nabla^2 \Phi = 0, \quad \text{for } \mathbf{x} = (x, y)^\top \in \mathbb{R}^2, \quad -h < z < \eta(x, y, t). \quad (1)$$

The nonlinear boundary conditions at $z = \eta(x, y, t)$ are the kinematic condition

$$\eta_t + \Phi_x \eta_x + \Phi_y \eta_y = \Phi_z, \quad (2)$$

and the dynamic condition

$$\Phi_t + \frac{1}{2} |\nabla \Phi|^2 + g\eta + \frac{\mathcal{D}}{\rho} \mathcal{F} = 0, \quad (3)$$

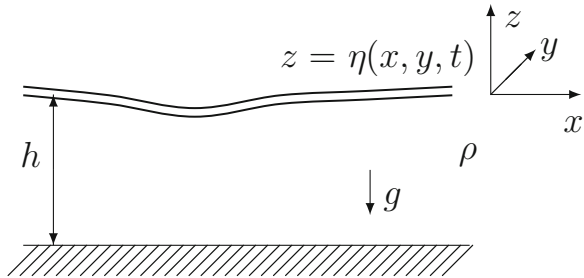
where

$$\begin{aligned} \mathcal{F} = & \frac{2}{\sqrt{\mathcal{A}}} \left[\partial_x \left(\frac{1 + \eta_y^2}{\sqrt{\mathcal{A}}} \partial_x \mathcal{H} \right) - \partial_x \left(\frac{\eta_x \eta_y}{\sqrt{\mathcal{A}}} \partial_y \mathcal{H} \right) - \partial_y \left(\frac{\eta_x \eta_y}{\sqrt{\mathcal{A}}} \partial_x \mathcal{H} \right) \right. \\ & \left. + \partial_y \left(\frac{1 + \eta_x^2}{\sqrt{\mathcal{A}}} \partial_y \mathcal{H} \right) \right] + 4\mathcal{H}^3 - 4\mathcal{H} \mathcal{H}', \end{aligned}$$

with

$$\mathcal{A} = 1 + \eta_x^2 + \eta_y^2, \quad \mathcal{H} = \frac{1}{\mathcal{A}^2} (\eta_{xx} \eta_{yy} - \eta_{xy}^2),$$

Fig. 1 Sketch of the hydroelastic problem



$$\mathcal{H} = \frac{1}{2\mathcal{A}^{3/2}} \left[(1 + \eta_y^2)\eta_{xx} - 2\eta_{xy}\eta_x\eta_y + (1 + \eta_x^2)\eta_{yy} \right].$$

The additional term \mathcal{F} in (3) represents the nonlinear bending force exerted by the ice sheet onto the fluid surface, as derived by Plotnikov and Toland [34]. It is also a conservative term and thus can be cast into a Hamiltonian formulation as shown below. Two simpler expressions of this bending force have been commonly used in the literature; a linear one based on Euler–Bernoulli theory [3, 24, 33, 37],

$$\mathcal{F} = \eta_{xxxx} + 2\eta_{xxyy} + \eta_{yyyy},$$

and a nonlinear one based on Kirchhoff–Love theory [4, 17, 29, 32]. The system is completed with the boundary condition at the bottom,

$$\Phi_z = 0, \quad \text{at } z = -h. \quad (4)$$

In the infinite-depth limit ($h \rightarrow \infty$), Eq. (4) is replaced by

$$|\nabla\Phi| \rightarrow 0, \quad \text{as } z \rightarrow -\infty.$$

If $\mathcal{D} = 0$, these are the classical governing equations for the gravity water wave problem [27].

Hereinafter, subscripts are also used as shorthand notation for partial or variational derivatives (e.g. $\Phi_t = \partial_t\Phi$). The vertical bars denote either a vector norm (when applied to a vector) or a complex modulus (when applied to a complex scalar function). The constant \mathcal{D} is the coefficient of flexural rigidity for the ice sheet, ρ the density of the fluid and g the acceleration due to gravity. The dynamic condition (3) stems from the Bernoulli equation [34]. The inertia of the thin elastic plate is neglected, so the plate acceleration term is not considered here [37]. We also assume that the elastic plate is not pre-stressed and neglect plate stretching.

The dispersion relation for the linearized problem with solutions of the form $e^{i(\mathbf{k}\cdot\mathbf{x}-\omega t)}$ is

$$c^2 = \left(\frac{g}{k} + \frac{\mathcal{D}k^3}{\rho} \right) \tanh(hk), \quad (5)$$

where $k = |\mathbf{k}|$ and $c = \omega/k$ is the phase speed. It can be shown that the phase speed $c(\mathbf{k})$ has a minimum c_{\min} at $\mathbf{k} = \mathbf{k}_{\min}$ for any parameter values [32, 37]. At this minimum, the phase velocity and group velocity are equal. Another critical speed in finite depth is the long-wave limit $c_0 = \sqrt{gh}$ as $k \rightarrow 0$.

The total energy

$$H = \frac{1}{2} \iint_{-\infty}^{\infty} \int_{-h}^{\eta} |\nabla\Phi|^2 dz dy dx + \frac{1}{2} \iint_{-\infty}^{\infty} \left[g\eta^2 + \frac{4\mathcal{D}}{\rho} \mathcal{H}^2 \sqrt{\mathcal{A}} \right] dy dx, \quad (6)$$

together with the impulse (or momentum) vector

$$I = \iint_{-\infty}^{\infty} \int_{-h}^{\eta} \nabla_{\mathbf{x}} \Phi \, dz dy dx,$$

where $\nabla_{\mathbf{x}} = (\partial_x, \partial_y)^\top$, and the volume (or mass)

$$V = \iint_{-\infty}^{\infty} \eta \, dy dx, \quad (7)$$

are invariants of motion for (1)–(4). The first integral in (6) represents kinetic energy, while the second integral represents potential energy due to gravity and elasticity.

2.2 Hamiltonian Formulation

Following Zakharov [45] and Craig and Sulem [14], we can reduce the dimensionality of the Laplace problem (1)–(4) by introducing $\xi(x, y, t) = \Phi(x, y, \eta(x, y, t), t)$, the trace of the velocity potential on $z = \eta(x, y, t)$, together with the DNO

$$G(\eta)\xi = (-\nabla_{\mathbf{x}}\eta, 1)^\top \cdot \nabla\Phi|_{z=\eta}, \quad (8)$$

which is the singular integral operator that takes Dirichlet data ξ on $z = \eta(x, y, t)$, solves the Laplace equation (1) for Φ subject to (4), and returns the corresponding Neumann data (i.e. the normal fluid velocity there).

In terms of these boundary variables, Eqs. (1)–(4) can be rewritten as

$$\eta_t = G(\eta)\xi, \quad (9)$$

$$\begin{aligned} \xi_t = & -\frac{1}{2(1 + |\nabla_{\mathbf{x}}\eta|^2)} \left[|\nabla_{\mathbf{x}}\xi|^2 - (G(\eta)\xi)^2 - 2(G(\eta)\xi)\nabla_{\mathbf{x}}\xi \cdot \nabla_{\mathbf{x}}\eta \right. \\ & \left. + |\nabla_{\mathbf{x}}\xi|^2 |\nabla_{\mathbf{x}}\eta|^2 - (\nabla_{\mathbf{x}}\xi \cdot \nabla_{\mathbf{x}}\eta)^2 \right] - g\eta - \frac{\mathcal{D}}{\rho} \mathcal{F}, \end{aligned} \quad (10)$$

which are Hamiltonian equations for the canonically conjugate variables η and ξ , extending Zakharov's formulation of the water wave problem to flexural-gravity waves [21–23]. Equations (9) and (10) have the canonical form

$$\begin{pmatrix} \eta_t \\ \xi_t \end{pmatrix} = J \begin{pmatrix} H_\eta \\ H_\xi \end{pmatrix} = \begin{pmatrix} 0 & 1 \\ -1 & 0 \end{pmatrix} \begin{pmatrix} H_\eta \\ H_\xi \end{pmatrix}, \quad (11)$$

whose Hamiltonian

$$H = \frac{1}{2} \iint_{-\infty}^{\infty} \left[\xi G(\eta)\xi + g\eta^2 + \frac{4\mathcal{D}}{\rho} \mathcal{H}^2 \sqrt{\mathcal{A}} \right] dy dx, \quad (12)$$

corresponds to the total energy (6).

The present Hamiltonian formulation involving the DNO can be extended to account for internal waves propagating e.g. along an interface between two fluid regions [5, 9, 11, 12] and for variable topography at the bottom of the fluid domain [6, 7, 20]. However, these effects will not be considered here.

2.3 Dirichlet–Neumann Operator

In light of its analyticity properties [13], the DNO can be expressed as a convergent Taylor series expansion in η ,

$$G(\eta) = \sum_{j=0}^{\infty} G_j(\eta), \quad (13)$$

where each term G_j can be determined recursively [14, 31, 44]. More specifically, for $j = 2r > 0$,

$$\begin{aligned} G_{2r}(\eta) &= \frac{1}{(2r)!} G_0 (|D_{\mathbf{x}}|^2)^{r-1} D_{\mathbf{x}} \cdot \eta^{2r} D_{\mathbf{x}} \\ &\quad - \sum_{s=0}^{r-1} \frac{1}{(2(r-s))!} (|D_{\mathbf{x}}|^2)^{r-s} \eta^{2(r-s)} G_{2s}(\eta) \\ &\quad - \sum_{s=0}^{r-1} \frac{1}{(2(r-s)-1)!} G_0 (|D_{\mathbf{x}}|^2)^{r-s-1} \eta^{2(r-s)-1} G_{2s+1}(\eta), \end{aligned} \quad (14)$$

and, for $j = 2r - 1 > 0$,

$$\begin{aligned} G_{2r-1}(\eta) &= \frac{1}{(2r-1)!} (|D_{\mathbf{x}}|^2)^{r-1} D_{\mathbf{x}} \cdot \eta^{2r-1} D_{\mathbf{x}} \\ &\quad - \sum_{s=0}^{r-1} \frac{1}{(2(r-s)-1)!} G_0 (|D_{\mathbf{x}}|^2)^{r-s-1} \eta^{2(r-s)-1} G_{2s}(\eta) \\ &\quad - \sum_{s=0}^{r-2} \frac{1}{(2(r-s-1))!} (|D_{\mathbf{x}}|^2)^{r-s-1} \eta^{2(r-s-1)} G_{2s+1}(\eta), \end{aligned} \quad (15)$$

where $D_{\mathbf{x}} = -i\nabla_{\mathbf{x}}$ and $G_0 = |D_{\mathbf{x}}| \tanh(h|D_{\mathbf{x}}|)$ are Fourier multiplier operators ($D_{\mathbf{x}}$ is defined in such a way that its Fourier symbol is \mathbf{k} and thus $|D_{\mathbf{x}}|$ corresponds to $|\mathbf{k}| = k$). In the infinite-depth limit ($h \rightarrow \infty$), G_0 reduces to $|D_{\mathbf{x}}|$ [21]. Similar expansions of the DNO can be derived in the presence of an interface between two fluid layers [5, 12, 19] and for variable bottom topography [6, 20].

3 Modulational Regime

We now present the derivation of weakly nonlinear models for small-amplitude waves in the modulational regime. For this purpose, we apply a Hamiltonian perturbation approach [5, 6, 8, 10], which is especially suitable for the present Hamiltonian formulation of the flexural-gravity wave problem. An advantage of this approach is that it naturally associates a Hamiltonian to the equations of motion at each order of approximation, although we restrict ourselves to approximations up to the cubic order of nonlinearity in the present paper. Long-wave models can be treated in a similar way [23] but they will not be examined here. Changing variables through canonical transformations and expanding the Hamiltonian are the main ingredients of this approach. We distinguish two cases: finite and infinite depth.

3.1 Finite Depth

3.1.1 Canonical Transformations

The first step is a normal decomposition of the first-harmonic waves, and here we extend the approach of Craig et al. [8, 10] by accounting for higher harmonics according to Stokes' expansion, as assumed in the multiple-scale method [3, 13, 15, 16, 30, 38, 40]. This translates into

$$\begin{aligned} \eta &= \frac{1}{\sqrt{2}} a^{-1}(D_{\mathbf{x}})(v + \bar{v}) + \tilde{\eta} + \eta_2 + \dots, & \tilde{\eta} &= \mathbb{P}_0 \eta, & \eta_2 &= \mathbb{P}_2 \eta, \\ \xi &= -\frac{i}{\sqrt{2}} a(D_{\mathbf{x}})(v - \bar{v}) + \tilde{\xi} + \xi_2 + \dots, & \tilde{\xi} &= \mathbb{P}_0 \xi, & \xi_2 &= \mathbb{P}_2 \xi, \end{aligned} \quad (16)$$

where

$$a(D_{\mathbf{x}}) = \sqrt[4]{\frac{g + \mathcal{D}|D_{\mathbf{x}}|^4/\rho}{G_0(D_{\mathbf{x}})}},$$

$(\tilde{\eta}, \tilde{\xi})$ are the zeroth harmonics representing the induced mean flow, and (η_2, ξ_2) the second harmonics. The overbar represents complex conjugation and $\mathbb{P}_0, \mathbb{P}_2$ are the projections that associate to (η, ξ) their zeroth- and second-harmonic components respectively. Higher harmonics can be taken into account but it is sufficient to consider only up to the second ones for the purposes of deriving the cubic NLS and DS equations in the present paper. As will be made clearer later, we use the terminology “first harmonics” to refer to the solution's components with wavenumbers centered around the fundamental (or carrier), “second harmonics” to those with wavenumbers centered around twice the fundamental, and so on.

The new variables $(v, \bar{v}, \eta_2, \xi_2, \tilde{\eta}, \tilde{\xi})^\top$ are expressed in terms of $(\eta, \xi)^\top$ as

$$\begin{pmatrix} v \\ \bar{v} \\ \eta_2 \\ \xi_2 \\ \tilde{\eta} \\ \tilde{\xi} \end{pmatrix} = A_1 \begin{pmatrix} \eta \\ \xi \end{pmatrix} = \frac{1}{\sqrt{2}} \begin{pmatrix} a(D_x)(\mathbb{I} - \mathbb{P}_0 - \mathbb{P}_2) & ia^{-1}(D_x)(\mathbb{I} - \mathbb{P}_0 - \mathbb{P}_2) \\ a(D_x)(\mathbb{I} - \mathbb{P}_0 - \mathbb{P}_2) & -ia^{-1}(D_x)(\mathbb{I} - \mathbb{P}_0 - \mathbb{P}_2) \\ \sqrt{2}\mathbb{P}_2 & 0 \\ 0 & \sqrt{2}\mathbb{P}_2 \\ \sqrt{2}\mathbb{P}_0 & 0 \\ 0 & \sqrt{2}\mathbb{P}_0 \end{pmatrix} \begin{pmatrix} \eta \\ \xi \end{pmatrix},$$

where \mathbb{I} denotes the identity operator. Accordingly, the symplectic structure of the system is changed to $J_1 = A_1 J A_1^\top$ [5, 8] and the equations of motion become

$$\begin{pmatrix} v_t \\ \bar{v}_t \\ \eta_{2t} \\ \xi_{2t} \\ \tilde{\eta}_t \\ \tilde{\xi}_t \end{pmatrix} = J_1 \begin{pmatrix} H_v \\ H_{\bar{v}} \\ H_{\eta_2} \\ H_{\xi_2} \\ H_{\tilde{\eta}} \\ H_{\tilde{\xi}} \end{pmatrix} = \begin{pmatrix} 0 & -i(\mathbb{I} - \mathbb{P}_0 - \mathbb{P}_2) & 0 & 0 & 0 & 0 \\ i(\mathbb{I} - \mathbb{P}_0 - \mathbb{P}_2) & 0 & 0 & 0 & 0 & 0 \\ 0 & 0 & 0 & \mathbb{P}_2 & 0 & 0 \\ 0 & 0 & -\mathbb{P}_2 & 0 & 0 & 0 \\ 0 & 0 & 0 & 0 & 0 & \mathbb{P}_0 \\ 0 & 0 & 0 & 0 & -\mathbb{P}_0 & 0 \end{pmatrix} \begin{pmatrix} H_v \\ H_{\bar{v}} \\ H_{\eta_2} \\ H_{\xi_2} \\ H_{\tilde{\eta}} \\ H_{\tilde{\xi}} \end{pmatrix},$$

given the fact that $\mathbb{P}_0^2 = \mathbb{P}_0$ and similarly for \mathbb{P}_2 . By also decomposing the second harmonics into normal modes,

$$\eta_2 = \frac{1}{\sqrt{2}} a^{-1}(D_x)(v_2 + \bar{v}_2), \quad \xi_2 = -\frac{i}{\sqrt{2}} a(D_x)(v_2 - \bar{v}_2),$$

we obtain

$$\begin{pmatrix} v_t \\ \bar{v}_t \\ v_{2t} \\ \bar{v}_{2t} \\ \tilde{\eta}_t \\ \tilde{\xi}_t \end{pmatrix} = J_2 \begin{pmatrix} H_v \\ H_{\bar{v}} \\ H_{v_2} \\ H_{\bar{v}_2} \\ H_{\tilde{\eta}} \\ H_{\tilde{\xi}} \end{pmatrix},$$

where

$$J_2 = \begin{pmatrix} 0 & -i(\mathbb{I} - \mathbb{P}_0 - \mathbb{P}_2) & 0 & 0 & 0 & 0 \\ i(\mathbb{I} - \mathbb{P}_0 - \mathbb{P}_2) & 0 & 0 & 0 & 0 & 0 \\ 0 & 0 & \frac{1}{2}(a\mathbb{P}_2 a^{-1} - a^{-1}\mathbb{P}_2 a) & -\frac{1}{2}(a\mathbb{P}_2 a^{-1} + a^{-1}\mathbb{P}_2 a) & 0 & 0 \\ 0 & 0 & \frac{1}{2}(a\mathbb{P}_2 a^{-1} + a^{-1}\mathbb{P}_2 a) & -\frac{1}{2}(a\mathbb{P}_2 a^{-1} - a^{-1}\mathbb{P}_2 a) & 0 & 0 \\ 0 & 0 & 0 & 0 & 0 & \mathbb{P}_0 \\ 0 & 0 & 0 & 0 & 0 & -\mathbb{P}_0 \end{pmatrix}.$$

If higher harmonics were to be considered, this would increase the size of the system of equations. These higher harmonics can also be expressed in terms of $(\eta, \xi)^\top$ by using the associated projections as in (16).

The next step introduces the modulational Ansatz

$$v = \varepsilon u(\mathbf{X}, t)e^{i\mathbf{k}_0 \cdot \mathbf{x}}, \quad \bar{v} = \varepsilon \bar{u}(\mathbf{X}, t)e^{-i\mathbf{k}_0 \cdot \mathbf{x}}, \quad (17)$$

$$v_2 = \varepsilon^2 u_2(\mathbf{X}, t)e^{2i\mathbf{k}_0 \cdot \mathbf{x}}, \quad \bar{v}_2 = \varepsilon^2 \bar{u}_2(\mathbf{X}, t)e^{-2i\mathbf{k}_0 \cdot \mathbf{x}}, \quad (18)$$

in the spirit of Stokes' expansion, together with

$$\tilde{\eta} = \varepsilon^\alpha \eta_0(\mathbf{X}, t), \quad \tilde{\xi} = \varepsilon^\beta \xi_0(\mathbf{X}, t), \quad (19)$$

where the exponents $\beta > 1$ and $\alpha = \beta + 1$ are dependent on whether the depth is finite or infinite [8]. This implies that we look for solutions in the form of quasi-monochromatic waves with nonzero carrier wavenumber $\mathbf{k}_0 = (k_x, k_y)^\top$ and with slowly varying amplitude depending on $\mathbf{X} = \varepsilon \mathbf{x}$. Wave steepness is measured by the small parameter $\varepsilon \sim |\mathbf{k}_0|a_0 \ll 1$ where a_0 is a characteristic wave amplitude. In [8, 10, 21, 23], the second harmonics were assumed to be of higher order than $O(\varepsilon^2)$ and thus did not contribute to the level of approximation considered. Such a regime may be interpreted as that for weakly nonlinear waves which are very close to being monochromatic (or equivalently for a very narrow-banded wave spectrum centered around \mathbf{k}_0). In the present case, these second harmonics give contributions, albeit small.

The system is now determined by the slowly varying amplitudes

$$\begin{pmatrix} u \\ \bar{u} \\ u_2 \\ \bar{u}_2 \\ \eta_0 \\ \xi_0 \end{pmatrix} = A_3 \begin{pmatrix} v \\ \bar{v} \\ v_2 \\ \bar{v}_2 \\ \tilde{\eta} \\ \tilde{\xi} \end{pmatrix} = \begin{pmatrix} \varepsilon^{-1}e^{-i\mathbf{k}_0 \cdot \mathbf{x}} & 0 & 0 & 0 & 0 & 0 \\ 0 & \varepsilon^{-1}e^{i\mathbf{k}_0 \cdot \mathbf{x}} & 0 & 0 & 0 & 0 \\ 0 & 0 & \varepsilon^{-2}e^{-2i\mathbf{k}_0 \cdot \mathbf{x}} & 0 & 0 & 0 \\ 0 & 0 & 0 & \varepsilon^{-2}e^{2i\mathbf{k}_0 \cdot \mathbf{x}} & 0 & 0 \\ 0 & 0 & 0 & 0 & \varepsilon^{-\alpha} & 0 \\ 0 & 0 & 0 & 0 & 0 & \varepsilon^{-\beta} \end{pmatrix} \begin{pmatrix} v \\ \bar{v} \\ v_2 \\ \bar{v}_2 \\ \tilde{\eta} \\ \tilde{\xi} \end{pmatrix},$$

whose evolution equations read

$$\begin{pmatrix} u_t \\ \bar{u}_t \\ u_{2t} \\ \bar{u}_{2t} \\ \eta_{0t} \\ \xi_{0t} \end{pmatrix} = J_3 \begin{pmatrix} H_u \\ H_{\bar{u}} \\ H_{u_2} \\ H_{\bar{u}_2} \\ H_{\eta_0} \\ H_{\xi_0} \end{pmatrix}, \quad (20)$$

where

$$J_3 = \varepsilon^2 A_3 J_2 A_3^\top = \varepsilon^2 \begin{pmatrix} 0 & \mathcal{J}_{12} & 0 & 0 & 0 & 0 \\ \mathcal{J}_{21} & 0 & 0 & 0 & 0 & 0 \\ 0 & 0 & 0 & \mathcal{J}_{34} & 0 & 0 \\ 0 & 0 & \mathcal{J}_{43} & 0 & 0 & 0 \\ 0 & 0 & 0 & 0 & 0 & \varepsilon^{-\alpha-\beta} \mathbb{P}_0 \\ 0 & 0 & 0 & 0 & -\varepsilon^{-\alpha-\beta} \mathbb{P}_0 & 0 \end{pmatrix},$$

and

$$\begin{aligned} \mathcal{J}_{12} &= -i\varepsilon^{-2} e^{-i\mathbf{k}_0 \cdot \mathbf{x}} (\mathbb{I} - \mathbb{P}_0 - \mathbb{P}_2)(e^{i\mathbf{k}_0 \cdot \mathbf{x}}), & \mathcal{J}_{21} &= \overline{\mathcal{J}_{12}}, \\ \mathcal{J}_{34} &= -i\varepsilon^{-4} e^{-2i\mathbf{k}_0 \cdot \mathbf{x}} \mathbb{P}_2(e^{2i\mathbf{k}_0 \cdot \mathbf{x}}), & \mathcal{J}_{43} &= \overline{\mathcal{J}_{34}}. \end{aligned}$$

Note that the additional factor ε^2 in J_3 is due to the spatial rescaling $\mathbf{x} \rightarrow \mathbf{X}$ [5, 8]. This new symplectic structure reduces to

$$J_3 = \begin{pmatrix} 0 & -i & 0 & 0 & 0 & 0 \\ i & 0 & 0 & 0 & 0 & 0 \\ 0 & 0 & 0 & -i\varepsilon^{-2} & 0 & 0 \\ 0 & 0 & i\varepsilon^{-2} & 0 & 0 & 0 \\ 0 & 0 & 0 & 0 & 0 & \varepsilon^{2-\alpha-\beta} \\ 0 & 0 & 0 & 0 & -\varepsilon^{2-\alpha-\beta} & 0 \end{pmatrix},$$

when applied to a homogenized Hamiltonian in terms of functions of \mathbf{X} alone, as described next.

3.1.2 Expansion of the Hamiltonian

The modulational Ansatz (17)–(19) also introduces the small parameter ε in the expression of the Hamiltonian (12) which can then be expanded in powers of ε , by using the Taylor series expansion (13) of the DNO. The mean-flow exponents are set to $\alpha = 2$ and $\beta = 1$, as determined in [8] for finite depth. Up to order $O(\varepsilon^2)$, we find

$$\begin{aligned} H &= \iint_{-\infty}^{\infty} \left[\frac{1}{2} \bar{u} \left(\omega(\mathbf{k}_0) + \varepsilon \nabla_{\mathbf{k}} \omega(\mathbf{k}_0) \cdot D_{\mathbf{X}} + \frac{\varepsilon^2}{2} \partial_{k_j k_\ell}^2 \omega(\mathbf{k}_0) D_{X_j X_\ell}^2 \right) u + \text{c.c.} \right. \\ &\quad + \varepsilon^2 \omega(2\mathbf{k}_0) |u_2|^2 + \varepsilon^2 \alpha_3(\mathbf{k}_0) |u|^4 + \varepsilon^2 \alpha_2(\mathbf{k}_0) \left(u^2 \bar{u}_2 + \bar{u}^2 u_2 \right) \\ &\quad \left. + \varepsilon^2 \left(i\mathbf{k}_0 \cdot D_{\mathbf{X}} \xi_0 + \alpha_1(\mathbf{k}_0) \eta_0 \right) |u|^2 + \frac{\varepsilon^2}{2} \left(h \xi_0 |D_{\mathbf{X}}|^2 \xi_0 + g \eta_0^2 \right) \right] dY dX + O(\varepsilon^3), \quad (21) \end{aligned}$$

where c.c. stands for the complex conjugate of all the preceding terms on the right-hand side of the equation, and

$$\begin{aligned}\alpha_1(\mathbf{k}_0) &= \frac{1}{2}a^2(\mathbf{k}_0)\left(|\mathbf{k}_0|^2 - G_0^2(\mathbf{k}_0)\right), \\ \alpha_2(\mathbf{k}_0) &= \frac{1}{2\sqrt{2}}a(2\mathbf{k}_0)\left(2|\mathbf{k}_0|^2 - G_0(\mathbf{k}_0)G_0(2\mathbf{k}_0)\right) \\ &\quad + \frac{1}{4\sqrt{2}}a^{-1}(2\mathbf{k}_0)a^2(\mathbf{k}_0)\left(|\mathbf{k}_0|^2 + G_0^2(\mathbf{k}_0)\right), \\ \alpha_3(\mathbf{k}_0) &= \frac{1}{4}G_0(\mathbf{k}_0)\left(G_0(\mathbf{k}_0)G_0(2\mathbf{k}_0) - |\mathbf{k}_0|^2\right) \\ &\quad - \frac{5\mathcal{D}}{8\rho}\left(k_x^6 + k_y^6 + 3k_x^4k_y^2 + 3k_x^2k_y^4\right)a^{-4}(\mathbf{k}_0).\end{aligned}$$

The coefficient

$$\omega(\mathbf{k}) = \sqrt{G_0(k)(g + \mathcal{D}k^4/\rho)},$$

denotes the linear dispersion relation in terms of the angular frequency and the indices $j, \ell = \{1, 2\}$ refer to the two horizontal directions. The scale separation lemma of Craig et al. [6] is applied to homogenize the fast oscillations in \mathbf{x} , so that four-wave resonant terms are retained and non-resonant terms are eliminated. Note the zeroth- and second-harmonic contributions to this order of approximation in (21).

The Hamiltonian (21) can be further simplified by subtracting a multiple of the wave action

$$M = \iint_{-\infty}^{\infty} |u|^2 dYdX,$$

together with a (scalar) multiple of the impulse

$$\begin{aligned}I &= \iint_{-\infty}^{\infty} \eta \nabla_{\mathbf{x}} \xi dydx, \\ &= \iint_{-\infty}^{\infty} \left[\mathbf{k}_0 |u|^2 + \frac{\varepsilon}{2} (\bar{u} D_{\mathbf{X}} u + u \overline{D_{\mathbf{X}} u}) + 2\varepsilon^2 \mathbf{k}_0 |u_2|^2 + i\varepsilon^2 \eta_0 D_{\mathbf{X}} \xi_0 \right] dYdX,\end{aligned}$$

so that it takes the “renormalized” form

$$\begin{aligned}\hat{H} &= H - \nabla_{\mathbf{k}} \omega(\mathbf{k}_0) \cdot I - \left(\omega(\mathbf{k}_0) - \mathbf{k}_0 \cdot \nabla_{\mathbf{k}} \omega(\mathbf{k}_0) \right) M, \\ &= \varepsilon^2 \iint_{-\infty}^{\infty} \left[\frac{1}{2} \partial_{k_j k_\ell}^2 \omega(\mathbf{k}_0) \bar{u} D_{X_j X_\ell}^2 u + \left(\omega(2\mathbf{k}_0) - 2\mathbf{k}_0 \cdot \nabla_{\mathbf{k}} \omega(\mathbf{k}_0) \right) |u_2|^2 \right]\end{aligned}$$

$$\begin{aligned}
& + \alpha_3(\mathbf{k}_0)|u|^4 + \alpha_2(\mathbf{k}_0)\left(u^2\bar{u}_2 + \bar{u}^2u_2\right) + \left(\mathbf{i}\mathbf{k}_0 \cdot D_{\mathbf{X}}\xi_0 + \alpha_1(\mathbf{k}_0)\eta_0\right)|u|^2 \\
& + \frac{1}{2}h\xi_0|D_{\mathbf{X}}|^2\xi_0 + \frac{1}{2}g\eta_0^2 - \mathbf{i}\nabla_{\mathbf{k}}\omega(\mathbf{k}_0) \cdot \eta_0 D_{\mathbf{X}}\xi_0 \Big] dYdX + O(\varepsilon^3). \quad (22)
\end{aligned}$$

The quantities I and M are conserved by the system, at least at the level of approximation considered. Therefore, they Poisson commute with H and do not modify its symplectic structure [5, 8]. The subtraction of a multiple of M from H reflects the fact that our approximation of the problem is phase invariant, while the subtraction of $\nabla_{\mathbf{k}}\omega(\mathbf{k}_0) \cdot I$ is equivalent to changing the coordinate system into a reference frame moving with the group velocity $\nabla_{\mathbf{k}}\omega(\mathbf{k}_0)$.

3.1.3 DS System

By using (22), the equations of motion (20) reduce to

$$\begin{aligned}
\mathbf{i}u_\tau = & -\frac{1}{2}\partial_{k_j k_\ell}^2 \omega(\mathbf{k}_0)\partial_{X_j X_\ell}^2 u + 2\alpha_3(\mathbf{k}_0)|u|^2 u + 2\alpha_2(\mathbf{k}_0)\bar{u}u_2 \\
& + \left(\mathbf{i}\mathbf{k}_0 \cdot D_{\mathbf{X}}\xi_0 + \alpha_1(\mathbf{k}_0)\eta_0\right)u, \quad (23)
\end{aligned}$$

$$\varepsilon\eta_{0\tau} = h|D_{\mathbf{X}}|^2\xi_0 - \mathbf{k}_0 \cdot \nabla_{\mathbf{X}}|u|^2 + \nabla_{\mathbf{k}}\omega(\mathbf{k}_0) \cdot \nabla_{\mathbf{X}}\eta_0, \quad (24)$$

$$\varepsilon\xi_{0\tau} = -\left(g\eta_0 + \alpha_1(\mathbf{k}_0)|u|^2 - \nabla_{\mathbf{k}}\omega(\mathbf{k}_0) \cdot \nabla_{\mathbf{X}}\xi_0\right), \quad (25)$$

$$\mathbf{i}\varepsilon^2 u_{2\tau} = \left(\omega(2\mathbf{k}_0) - 2\mathbf{k}_0 \cdot \nabla_{\mathbf{k}}\omega(\mathbf{k}_0)\right)u_2 + \alpha_2(\mathbf{k}_0)u^2, \quad (26)$$

where $\tau = \varepsilon^2 t$. To lowest order in ε , the right-hand sides of (24)–(26) equal zero, hence

$$h|D_{\mathbf{X}}|^2\xi_0 - \mathbf{k}_0 \cdot \nabla_{\mathbf{X}}|u|^2 + \nabla_{\mathbf{k}}\omega(\mathbf{k}_0) \cdot \nabla_{\mathbf{X}}\eta_0 = 0, \quad (27)$$

and

$$\eta_0 = -\frac{1}{g}\alpha_1(\mathbf{k}_0)|u|^2 + \frac{1}{g}\nabla_{\mathbf{k}}\omega(\mathbf{k}_0) \cdot \nabla_{\mathbf{X}}\xi_0, \quad (28)$$

$$u_2 = \frac{\alpha_2(\mathbf{k}_0)}{2\mathbf{k}_0 \cdot \nabla_{\mathbf{k}}\omega(\mathbf{k}_0) - \omega(2\mathbf{k}_0)}u^2. \quad (29)$$

Then substituting (28)–(29) into (23) and (27) leads to the DS system

$$\begin{aligned}
\mathbf{i}u_\tau = & -\frac{1}{2}\partial_{k_j k_\ell}^2 \omega(\mathbf{k}_0)\partial_{X_j X_\ell}^2 u + \alpha_4(\mathbf{k}_0)|u|^2 u + \alpha_5(\mathbf{k}_0) \cdot u \nabla_{\mathbf{X}}\xi_0, \\
0 = & \mathcal{L}\xi_0 - \alpha_5(\mathbf{k}_0) \cdot \nabla_{\mathbf{X}}|u|^2, \quad (30)
\end{aligned}$$

where

$$\begin{aligned}\alpha_4(\mathbf{k}_0) &= \frac{2\alpha_2^2(\mathbf{k}_0)}{2\mathbf{k}_0 \cdot \nabla_{\mathbf{k}}\omega(\mathbf{k}_0) - \omega(2\mathbf{k}_0)} + 2\alpha_3(\mathbf{k}_0) - \frac{1}{g}\alpha_1^2(\mathbf{k}_0), \\ \alpha_5(\mathbf{k}_0) &= \mathbf{k}_0 + \frac{1}{g}\alpha_1(\mathbf{k}_0)\nabla_{\mathbf{k}}\omega(\mathbf{k}_0), \\ \mathcal{L} &= -h|\nabla_{\mathbf{x}}|^2 + \frac{1}{g}\left(\partial_{k_j}\omega(\mathbf{k}_0)\right)\left(\partial_{k_\ell}\omega(\mathbf{k}_0)\right)\partial_{x_j x_\ell}^2.\end{aligned}$$

As mentioned earlier, setting $\mathcal{D} = 0$ in (30) and in the subsequent envelope equations reduces them to models for surface gravity water waves.

3.1.4 NLS Equation

In the two-dimensional case, the DS system (30) simplifies to

$$\begin{aligned}iu_\tau + \frac{1}{2}\partial_k^2\omega(k_0)\partial_X^2u - \alpha_4(k_0)|u|^2u - \alpha_5(k_0)u\partial_X\xi_0 &= 0, \\ \left[-h + \frac{1}{g}\left(\partial_k\omega(k_0)\right)^2\right]\partial_X^2\xi_0 - \alpha_5(k_0)\partial_X|u|^2 &= 0.\end{aligned}$$

Integrating the second equation above with respect to X by assuming vanishing conditions at infinity (as is the case for solitary waves) gives

$$\partial_X\xi_0 = \frac{\alpha_5(k_0)}{\frac{1}{g}(\partial_k\omega(k_0))^2 - h}|u|^2, \quad (31)$$

and then substituting this into the first equation yields the NLS equation

$$iu_\tau + \lambda\partial_X^2u + \mu|u|^2u = 0, \quad (32)$$

where

$$\begin{aligned}\lambda &= \frac{1}{2}\partial_k^2\omega(k_0), \\ \mu &= -\alpha_4(k_0) - \frac{\alpha_5^2(k_0)}{\frac{1}{g}(\partial_k\omega(k_0))^2 - h}.\end{aligned}$$

The corresponding Hamiltonian (with respect to τ) reads

$$H = \int_{-\infty}^{\infty} \left(\lambda|\partial_Xu|^2 - \frac{1}{2}\mu|u|^4 \right) dX, \quad (33)$$

so that $u_\tau = -iH_{\bar{u}}$ and is obtained by inserting (28), (29), (31) in (22). For convenience, the hat notation is dropped from (33).

Similarly to the classical water wave problem in finite depth [1, 15], the coefficient μ of the nonlinear term may have two singularities at $(\partial_k \omega(k_0))^2 = gh$ and $\omega(2k_0)/(2k_0) = \partial_k \omega(k_0)$ corresponding to resonances between the zeroth and first harmonics and between the first and second harmonics, respectively. The former singularity occurs if the group velocity of the first harmonics equals the phase velocity of the zeroth harmonics (i.e. the long-wave limit c_0), while the latter singularity occurs if the same group velocity equals the phase velocity of the second harmonics. The presence of the first-harmonic group velocity $\partial_k \omega(k_0)$ in these singularities is related to the fact that the reference frame is moving with this velocity, as mentioned above. In the present problem, a natural choice for k_0 is k_{\min} . For a given value of h , the corresponding k_{\min} is found numerically where the dispersion relation (5) achieves its minimum c_{\min} . Figure 2 reveals that both $c(2k_{\min}) = \omega(2k_{\min})/(2k_{\min})$ and $c_0 = \sqrt{gh}$ tend to $c_{\min} = \partial_k \omega(k_{\min})$ as $h \rightarrow 0$. Therefore, the modulational regime becomes inadequate and the long-wave regime should be preferred in the shallow-water limit, as could be expected [23].

According to (16), the ice-sheet deflection can be expressed in terms of u as

$$\eta(X, \tau) = \frac{\varepsilon}{\sqrt{2}} [a^{-1}(k_0 + \varepsilon D_X)u(X, \tau)e^{ik_0 X/\varepsilon} + \text{c.c.}] + \frac{\varepsilon^2}{\sqrt{2}} [a^{-1}(2k_0 + \varepsilon D_X)u_2(X, \tau)e^{2ik_0 X/\varepsilon} + \text{c.c.}] + \varepsilon^2 \eta_0(X, \tau), \quad (34)$$

where u_2 is given by (29), and

$$\eta_0 = \frac{\alpha_1(k_0)h + k_0 \partial_k \omega(k_0)}{(\partial_k \omega(k_0))^2 - gh} |u|^2,$$

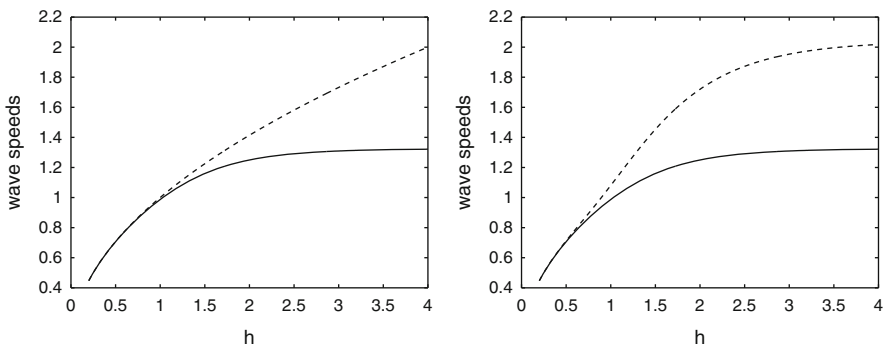


Fig. 2 Left panel: c_{\min} (solid line) and c_0 (dashed line) versus h . Right panel: c_{\min} (solid line) and $c(2k_{\min})$ (dashed line) versus h

by combining (28) with (31). The zeroth and second harmonics add corrections to the coefficients in the envelope equation for the first harmonics but also to the formula recovering the ice-sheet deflection. An expression similar to (34) holds for η in the three-dimensional case, with η_0 determined by (28) and the solution of the DS system. Equation (34) can be evaluated numerically by a pseudo-spectral method, which is a natural choice for computing such Fourier multipliers as a^{-1} [10, 14, 20, 21, 31, 44].

3.1.5 Soliton Solutions

In view of presenting numerical results, we non-dimensionalize the equations by using the characteristic length and velocity scales

$$\mathcal{L} = \left(\frac{\mathcal{D}}{\rho g} \right)^{1/4}, \quad \mathcal{V} = \left(\frac{\mathcal{D} g^3}{\rho} \right)^{1/8},$$

respectively, so that $g = 1$ and $\mathcal{D}/\rho = 1$ as a consequence [4, 29, 39].

The NLS equation (32) is of focusing type and thus admits stable soliton solutions traveling at the group velocity $\partial_k \omega(k_0)$ if $\lambda \mu > 0$ [18, 38]. The graphs of λ and μ for $k_0 = k_{\min}$ are shown in Fig. 3. We see that λ is increasing and always positive, while μ is decreasing and changes sign at the critical depth $h_c \simeq 36.75$. Accordingly, the NLS equation (32) is of focusing type if $h < h_c$ and defocusing if $h > h_c$. Because $\mu = 0$ at $h = h_c$, this implies that higher-order terms must be included in the equation, but we will not consider this situation here. In the linear Euler–Bernoulli case (by setting $\mathcal{D} = 0$ in α_3), we find $h_c \simeq 5.54$, which is close to the value $h_c \simeq 5.91$ reported by Milewski and Wang [30]. For a Kirchhoff–Love model of the ice sheet, Părău and Dias [32] found $h_c \simeq 7.63$, which is smaller than the present value for the Cosserat model. The fact that $\mu \rightarrow \infty$ as $h \rightarrow 0$ in Fig. 3 is consistent with the two resonances in the shallow-water limit as discussed in Sect. 3.1.4.

Since we are interested in solitary waves, the key parameters to be examined are the wave speed $c < c_{\min}$ and the water depth $h < h_c$. Figures 4 and 5 present a comparison of solitary wave profiles for various values of (c, h) , which are obtained from direct numerical simulations of (1)–(4) and from the exact NLS soliton solution

$$u(X, \tau) = \sqrt{2} u_0 \operatorname{sech} \left(u_0 \sqrt{\frac{\mu}{\lambda}} X \right) e^{i\mu u_0^2 \tau}, \quad (35)$$

which corresponds to solitary waves whose crests are stationary relative to their envelopes [2]. In the latter case, the ice-sheet deflection (34) is evaluated as

$$\begin{aligned} \eta(X, \tau) &= \frac{\varepsilon}{\sqrt{2}} \left[\operatorname{FT}^{-1} \left\{ a^{-1}(k_0 + \varepsilon K) \operatorname{FT}(u) \right\} e^{ik_0 X/\varepsilon} + \text{c.c.} \right] \\ &+ \frac{\varepsilon^2}{\sqrt{2}} \left[\operatorname{FT}^{-1} \left\{ a^{-1}(2k_0 + \varepsilon K) \operatorname{FT}(u_2) \right\} e^{2ik_0 X/\varepsilon} + \text{c.c.} \right] + \varepsilon^2 \eta_0(X, \tau), \end{aligned}$$

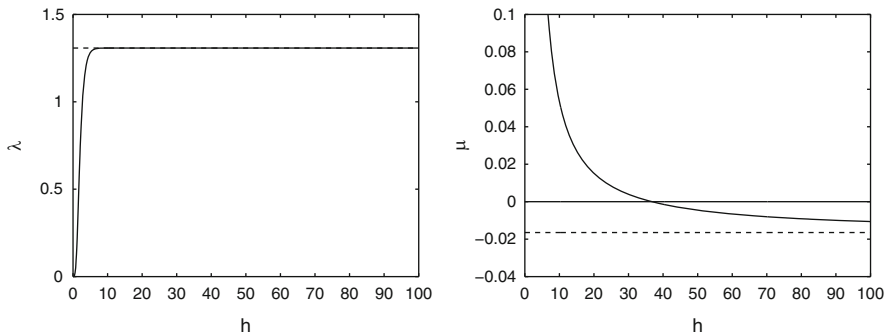


Fig. 3 NLS coefficients λ (left panel, solid line) and μ (right panel, solid line) versus h . As a reference, the corresponding values in the infinite-depth limit (see Sect. 3.2) are represented by a dashed line

where FT denotes the fast Fourier transform [10]. A number of 4096 grid points are typically used in our computations. For convenience, we set $\varepsilon = 1$ and only vary u_0 in (35) to match the fully nonlinear profile as closely as possible (which is equivalent to absorbing ε into u_0). The direct numerical simulations are based on a boundary-integral method with finite-difference approximations and the reader is referred to [21–23] for further details.

Overall there is a good agreement, especially regarding the relative amplitude of the central trough and the wavelength. The agreement is satisfactory even for moderately large wave amplitudes (compared to h , see Fig. 5), which is remarkable given the weakly nonlinear nature of the cubic NLS equation. The NLS prediction is able to capture well the main features, whether the solution is a localized or broader solitary wavepacket. This confirms in particular that the inclusion of the mean-flow component η_0 in (34) is crucial at reproducing well the vertical asymmetry of the solution. The second-harmonic corrections, however, are negligible according to the comparison of the two columns in Figs. 4 and 5. The left column of these figures shows results without second-harmonic contributions as in [23]. Only little improvement due to these second harmonics is noticeable in Fig. 5 for $h = 3.095$. Consistent with statements in Sect. 3.1.4, the agreement between numerical and NLS predictions slowly deteriorates as h decreases. We pay attention to the case $h = 3.095$ because it corresponds to Takizawa’s experiments on Lake Saroma (Japan) [39], where the ice thickness was 0.17 m and the water depth was 6.8 m. Waves were generated by moving a load (ski-doo snowmobile) at various speeds on top of the ice sheet. Wavelengths of order $O(10)$ m were observed. For $h = 3.095$, our results resemble some of his observations. We find similar wave profiles for larger depths.

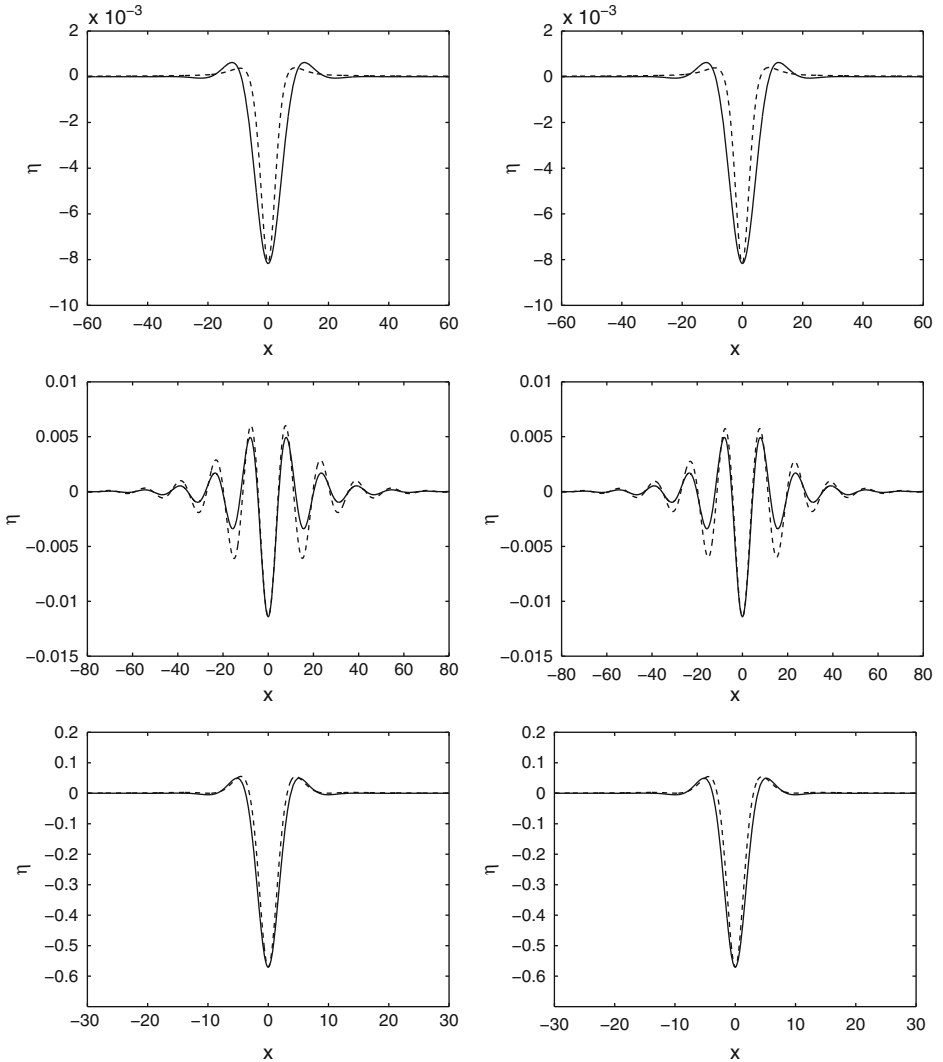


Fig. 4 Comparison of solitary wave profiles obtained from direct numerical simulations (*solid line*) and the NLS soliton (35) (*dashed line*) for $(c, h) = (0.7, 0.5), (0.985, 1)$ and $(0.9, 1.5)$ (from *top to bottom*). The *left and right columns* show the solutions without and with second-harmonic contributions, respectively

3.2 Infinite Depth

In this regime, the mean-flow exponents $\alpha = 3$ and $\beta = 2$ are larger than those in finite depth (see [8] for an explanation). As a consequence, the mean-flow terms do not contribute to the order of approximation being considered, and the renormalized

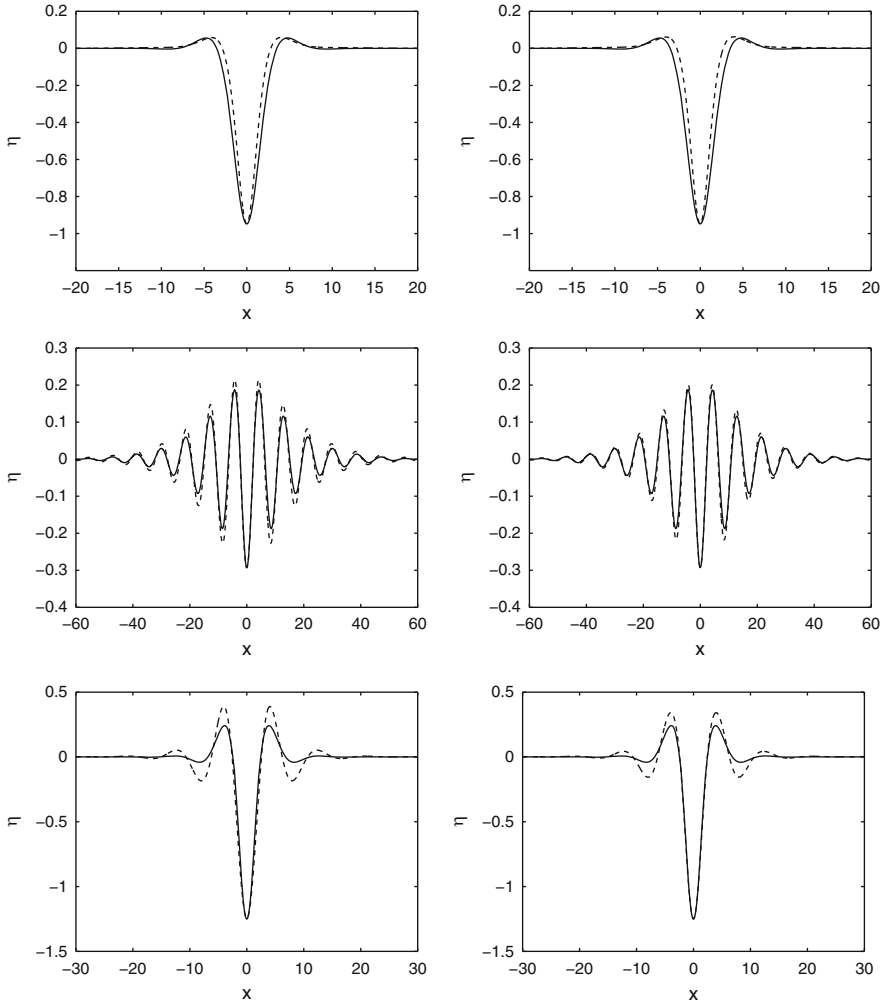


Fig. 5 Comparison of solitary wave profiles obtained from direct numerical simulations (*solid line*) and the NLS soliton (35) (*dashed line*) for $(c, h) = (0.658, 1.5)$, $(1.3, 3.095)$ and $(1.056, 3.095)$ (from *top to bottom*). The *left and right columns* show the solutions without and with second-harmonic contributions, respectively

Hamiltonian takes the form

$$\hat{H} = \varepsilon^2 \iint_{-\infty}^{\infty} \left[\frac{1}{2} \partial_{k_j k_\ell}^2 \omega(\mathbf{k}_0) \bar{u} D_{X_j X_\ell}^2 u + \left(\omega(2\mathbf{k}_0) - 2\mathbf{k}_0 \cdot \nabla_{\mathbf{k}} \omega(\mathbf{k}_0) \right) |u_2|^2 \right. \\ \left. + \left\{ \frac{1}{4} |\mathbf{k}_0|^3 - \frac{5\mathcal{D}}{8\rho} \left(k_x^6 + k_y^6 + 3k_x^4 k_y^2 + 3k_x^2 k_y^4 \right) a^{-4}(\mathbf{k}_0) \right\} |u|^4 \right]$$

$$+ \frac{1}{2\sqrt{2}} |\mathbf{k}_0|^2 a^{-1}(2\mathbf{k}_0) a^2(\mathbf{k}_0) \left(u^2 \bar{u}_2 + \bar{u}^2 u_2 \right) \Big] dYdX + O(\varepsilon^3). \quad (36)$$

The equations of motion (20) then become

$$\begin{aligned} iu_\tau = & -\frac{1}{2} \partial_{k_j k_\ell}^2 \omega(\mathbf{k}_0) \partial_{x_j x_\ell}^2 u + \frac{1}{\sqrt{2}} |\mathbf{k}_0|^2 a^{-1}(2\mathbf{k}_0) a^2(\mathbf{k}_0) \bar{u} u_2 \\ & + \left\{ \frac{1}{2} |\mathbf{k}_0|^3 - \frac{5\mathcal{D}}{4\rho} \left(k_x^6 + k_y^6 + 3k_x^4 k_y^2 + 3k_x^2 k_y^4 \right) a^{-4}(\mathbf{k}_0) \right\} |u|^2 u, \end{aligned} \quad (37)$$

$$\begin{aligned} i\varepsilon^2 u_{2\tau} = & \left(\omega(2\mathbf{k}_0) - 2\mathbf{k}_0 \cdot \nabla_{\mathbf{k}} \omega(\mathbf{k}_0) \right) u_2 + \frac{1}{2\sqrt{2}} |\mathbf{k}_0|^2 a^{-1}(2\mathbf{k}_0) a^2(\mathbf{k}_0) u^2, \\ \varepsilon^3 \eta_{0\tau} = & 0, \\ \varepsilon^3 \xi_{0\tau} = & 0, \end{aligned} \quad (38)$$

which confirms that the mean-flow contributions are negligible, while

$$u_2 = \frac{|\mathbf{k}_0|^2 a^{-1}(2\mathbf{k}_0) a^2(\mathbf{k}_0)}{2\sqrt{2} (2\mathbf{k}_0 \cdot \nabla_{\mathbf{k}} \omega(\mathbf{k}_0) - \omega(2\mathbf{k}_0))} u^2, \quad (39)$$

to lowest order by virtue of (38). Substituting (39) into (36) and (37) leads to the NLS equation

$$\begin{aligned} iu_\tau = & -\frac{1}{2} \partial_{k_j k_\ell}^2 \omega(\mathbf{k}_0) \partial_{x_j x_\ell}^2 u + \left\{ \frac{|\mathbf{k}_0|^4 a^{-2}(2\mathbf{k}_0) a^4(\mathbf{k}_0)}{4 (2\mathbf{k}_0 \cdot \nabla_{\mathbf{k}} \omega(\mathbf{k}_0) - \omega(2\mathbf{k}_0))} \right. \\ & \left. + \frac{1}{2} |\mathbf{k}_0|^3 - \frac{5\mathcal{D}}{4\rho} \left(k_x^6 + k_y^6 + 3k_x^4 k_y^2 + 3k_x^2 k_y^4 \right) a^{-4}(\mathbf{k}_0) \right\} |u|^2 u, \end{aligned} \quad (40)$$

whose Hamiltonian (with respect to τ) is

$$\begin{aligned} H = & \iint_{-\infty}^{\infty} \left[\frac{1}{2} \partial_{k_j k_\ell}^2 \omega(\mathbf{k}_0) \overline{(\partial_{x_j} u)} (\partial_{x_\ell} u) + \left\{ \frac{|\mathbf{k}_0|^4 a^{-2}(2\mathbf{k}_0) a^4(\mathbf{k}_0)}{8 (2\mathbf{k}_0 \cdot \nabla_{\mathbf{k}} \omega(\mathbf{k}_0) - \omega(2\mathbf{k}_0))} \right. \right. \\ & \left. \left. + \frac{1}{4} |\mathbf{k}_0|^3 - \frac{5\mathcal{D}}{8\rho} \left(k_x^6 + k_y^6 + 3k_x^4 k_y^2 + 3k_x^2 k_y^4 \right) a^{-4}(\mathbf{k}_0) \right\} |u|^4 \right] dYdX. \end{aligned}$$

In the two-dimensional case, we again obtain an NLS equation of the form (32), with Hamiltonian (33), where

$$\lambda = \frac{1}{2} \partial_k^2 \omega(k_0) = \frac{5\mathcal{D}k_0^3}{\rho \sqrt{gk_0 + \mathcal{D}k_0^5/\rho}} - \frac{(g + 5\mathcal{D}k_0^4/\rho)^2}{8(gk_0 + \mathcal{D}k_0^5/\rho)^{3/2}},$$

and

$$\mu = \frac{5\mathcal{D}k_0^7}{4\rho(g + \mathcal{D}k_0^4/\rho)} - \frac{k_0^3}{2} - \frac{k_0^3(g + \mathcal{D}k_0^4/\rho)}{4(2k_0\partial_k\omega(k_0) - \omega(2k_0))} \sqrt{\frac{2k_0}{g + 16\mathcal{D}k_0^4/\rho}}.$$

Without loss of generality, the carrier wavenumber $k_0 = k_x$ is assumed to be positive. Again the coefficient μ may have a singularity at $\omega(2k_0)/(2k_0) = \partial_k\omega(k_0)$ due to the first-second harmonic resonance, but the zeroth-first harmonic resonance is absent here since the mean flow does not come into play. The ice-sheet deflection can be recovered from u by using (34) as well, but without need for the higher-order $O(\varepsilon^3)$ contribution from η_0 .

In infinite depth [21, 37], the phase speed is minimum at

$$k_{\min} = \left(\frac{g\rho}{3\mathcal{D}}\right)^{1/4}.$$

After applying the same non-dimensionalization as in Sect. 3.1.5, we find that $\lambda\mu < 0$ if $k_0 = k_{\min}$ since

$$\lambda = \frac{3^{7/8}}{2} \simeq 1.307 > 0,$$

and

$$\mu = -\frac{3^{1/4}(41\sqrt{38} - 228)}{912(\sqrt{38} - 4)} \simeq -0.016 < 0.$$

Incidentally, the above-mentioned denominator in μ

$$\frac{\omega(2k_{\min})}{2k_{\min}} - \partial_k\omega(k_{\min}) = \frac{3^{5/8}(\sqrt{38} - 4)}{6} \simeq 0.717,$$

does not vanish, as also indicated in Fig. 2 for large h . Therefore, the NLS equation is of defocusing type and no soliton solutions exist in this limit. This result is consistent with the asymptotic behavior of λ and μ for finite depth as $h \rightarrow \infty$ (see Sect. 3.1.5). Previous studies using different methods of derivation and different models for the ice sheet (e.g. Kirchhoff–Love theory) also obtained a defocusing NLS equation in this regime [21, 29].

3.3 Exact Linear Dispersion

3.3.1 Finite Depth

As suggested in [10, 27, 41], the linear dispersive properties of envelope equations can be improved by retaining the exact linear dispersion relation rather than Taylor expanding it. For finite depth, a counterpart to (22) is

$$\begin{aligned}
\hat{H} &= H - \omega(\mathbf{k}_0)M, \\
&= \varepsilon^2 \iint_{-\infty}^{\infty} \left[\frac{1}{\varepsilon^2} \bar{u} \left(\omega(\mathbf{k}_0 + \varepsilon D_{\mathbf{X}}) - \omega(\mathbf{k}_0) \right) u + \omega(2\mathbf{k}_0) |u_2|^2 + \alpha_3(\mathbf{k}_0) |u|^4 \right. \\
&\quad \left. + \alpha_2(\mathbf{k}_0) \left(u^2 \bar{u}_2 + \bar{u}^2 u_2 \right) + \left(i\mathbf{k}_0 \cdot D_{\mathbf{X}} \xi_0 + \alpha_1(\mathbf{k}_0) \eta_0 \right) |u|^2 \right. \\
&\quad \left. + \frac{1}{2\varepsilon^2} \xi_0 G_0(\varepsilon D_{\mathbf{X}}) \xi_0 + \frac{1}{2} g \eta_0^2 \right] dY dX + O(\varepsilon^3), \tag{41}
\end{aligned}$$

and the corresponding evolution equations are

$$\begin{aligned}
iu_{\tau} &= \frac{1}{\varepsilon^2} \left(\omega(\mathbf{k}_0 + \varepsilon D_{\mathbf{X}}) - \omega(\mathbf{k}_0) \right) u + 2\alpha_3(\mathbf{k}_0) |u|^2 u + 2\alpha_2(\mathbf{k}_0) \bar{u} u_2 \\
&\quad + \left(i\mathbf{k}_0 \cdot D_{\mathbf{X}} \xi_0 + \alpha_1(\mathbf{k}_0) \eta_0 \right) u, \\
\varepsilon \eta_{0\tau} &= \frac{1}{\varepsilon^2} G_0(\varepsilon D_{\mathbf{X}}) \xi_0 - \mathbf{k}_0 \cdot \nabla_{\mathbf{X}} |u|^2, \\
\varepsilon \xi_{0\tau} &= - \left(g \eta_0 + \alpha_1(\mathbf{k}_0) |u|^2 \right), \\
i\varepsilon^2 u_{2\tau} &= \omega(2\mathbf{k}_0) u_2 + \alpha_2(\mathbf{k}_0) u^2.
\end{aligned}$$

By following the same procedure as in Sect. 3.1.3, we find the modified DS system

$$\begin{aligned}
iu_{\tau} &= \frac{1}{\varepsilon^2} \left(\omega(\mathbf{k}_0 + \varepsilon D_{\mathbf{X}}) - \omega(\mathbf{k}_0) \right) u + \left(2\alpha_3(\mathbf{k}_0) - \frac{2\alpha_2^2(\mathbf{k}_0)}{\omega(2\mathbf{k}_0)} - \frac{1}{g} \alpha_1^2(\mathbf{k}_0) \right) |u|^2 u \\
&\quad + u \mathbf{k}_0 \cdot \nabla_{\mathbf{X}} \xi_0, \\
0 &= \frac{1}{\varepsilon^2} G_0(\varepsilon D_{\mathbf{X}}) \xi_0 - \mathbf{k}_0 \cdot \nabla_{\mathbf{X}} |u|^2,
\end{aligned}$$

where

$$\eta_0 = -\frac{1}{g} \alpha_1(\mathbf{k}_0) |u|^2, \quad u_2 = -\frac{\alpha_2(\mathbf{k}_0)}{\omega(2\mathbf{k}_0)} u^2,$$

to lowest order. In the two-dimensional case, the second equation in this DS system can be solved for $\partial_X \xi_0$, hence

$$\partial_X \xi_0 = \varepsilon^2 k_0 G_0^{-1}(\varepsilon D_X) \partial_X^2 |u|^2.$$

Substituting this into the first equation yields the modified NLS equation

$$\begin{aligned} iu_\tau = & \frac{1}{\varepsilon^2} \left(\omega(k_0 + \varepsilon D_X) - \omega(k_0) \right) u + \left(2\alpha_3(k_0) - \frac{2\alpha_2^2(k_0)}{\omega(2k_0)} - \frac{1}{g} \alpha_1^2(k_0) \right) |u|^2 u \\ & + \varepsilon^2 k_0^2 u G_0^{-1} (\varepsilon D_X) \partial_X^2 |u|^2, \end{aligned}$$

with Hamiltonian

$$\begin{aligned} H = & \int_{-\infty}^{\infty} \left[\frac{1}{\varepsilon^2} \bar{u} \left(\omega(k_0 + \varepsilon D_X) - \omega(k_0) \right) u + \frac{1}{2} \left(2\alpha_3(k_0) - \frac{2\alpha_2^2(k_0)}{\omega(2k_0)} - \frac{1}{g} \alpha_1^2(k_0) \right) |u|^4 \right. \\ & \left. + \frac{1}{2} \varepsilon^2 k_0^2 |u|^2 G_0^{-1} (\varepsilon D_X) \partial_X^2 |u|^2 \right] dX, \end{aligned}$$

as derived from (41). Here again, these modified DS and NLS equations can be solved numerically by a pseudo-spectral method which is suitable for handling the Fourier multipliers ω and G_0 . Note that the operator $G_0^{-1} (\varepsilon D_X) \partial_X^2$ is well-defined, and in particular it is not singular at $k = 0$ as can be shown by a Taylor series expansion in ε .

3.3.2 Infinite Depth

For infinite depth, the renormalized Hamiltonian is given by

$$\begin{aligned} \hat{H} = & \varepsilon^2 \iint_{-\infty}^{\infty} \left[\frac{1}{\varepsilon^2} \bar{u} \left(\omega(\mathbf{k}_0 + \varepsilon D_{\mathbf{X}}) - \omega(\mathbf{k}_0) \right) u + \omega(2\mathbf{k}_0) |u_2|^2 \right. \\ & + \left\{ \frac{1}{4} |\mathbf{k}_0|^3 - \frac{5\mathcal{D}}{8\rho} \left(k_x^6 + k_y^6 + 3k_x^4 k_y^2 + 3k_x^2 k_y^4 \right) a^{-4}(\mathbf{k}_0) \right\} |u|^4 \\ & \left. + \frac{1}{2\sqrt{2}} |\mathbf{k}_0|^2 a^{-1}(2\mathbf{k}_0) a^2(\mathbf{k}_0) \left(u^2 \bar{u}_2 + \bar{u}^2 u_2 \right) \right] dY dX + O(\varepsilon^3), \end{aligned}$$

whose dynamics obeys

$$\begin{aligned} iu_\tau = & \frac{1}{\varepsilon^2} \left(\omega(\mathbf{k}_0 + \varepsilon D_{\mathbf{X}}) - \omega(\mathbf{k}_0) \right) u + \frac{1}{\sqrt{2}} |\mathbf{k}_0|^2 a^{-1}(2\mathbf{k}_0) a^2(\mathbf{k}_0) \bar{u} u_2 \\ & + \left\{ \frac{1}{2} |\mathbf{k}_0|^3 - \frac{5\mathcal{D}}{4\rho} \left(k_x^6 + k_y^6 + 3k_x^4 k_y^2 + 3k_x^2 k_y^4 \right) a^{-4}(\mathbf{k}_0) \right\} |u|^2 u, \quad (42) \end{aligned}$$

$$i\varepsilon^2 u_{2\tau} = \omega(2\mathbf{k}_0) u_2 + \frac{1}{2\sqrt{2}} |\mathbf{k}_0|^2 a^{-1}(2\mathbf{k}_0) a^2(\mathbf{k}_0) u^2. \quad (43)$$

Combining (42) and (43) as in Sect. 3.2 leads to the modified NLS equation

$$iu_\tau = \frac{1}{\varepsilon^2} \left(\omega(\mathbf{k}_0 + \varepsilon D_X) - \omega(\mathbf{k}_0) \right) u - \left\{ \frac{|\mathbf{k}_0|^4 a^{-2}(2\mathbf{k}_0) a^4(\mathbf{k}_0)}{4\omega(2\mathbf{k}_0)} - \frac{1}{2} |\mathbf{k}_0|^3 + \frac{5\mathcal{D}}{4\rho} \left(k_x^6 + k_y^6 + 3k_x^4 k_y^2 + 3k_x^2 k_y^4 \right) a^{-4}(\mathbf{k}_0) \right\} |u|^2 u,$$

such that

$$u_2 = - \frac{|\mathbf{k}_0|^2 a^{-1}(2\mathbf{k}_0) a^2(\mathbf{k}_0)}{2\sqrt{2}\omega(2\mathbf{k}_0)} u^2.$$

The corresponding Hamiltonian reads

$$H = \iint_{-\infty}^{\infty} \left[\frac{1}{\varepsilon^2} \bar{u} \left(\omega(\mathbf{k}_0 + \varepsilon D_X) - \omega(\mathbf{k}_0) \right) u - \left\{ \frac{|\mathbf{k}_0|^4 a^{-2}(2\mathbf{k}_0) a^4(\mathbf{k}_0)}{8\omega(2\mathbf{k}_0)} - \frac{1}{4} |\mathbf{k}_0|^3 + \frac{5\mathcal{D}}{8\rho} \left(k_x^6 + k_y^6 + 3k_x^4 k_y^2 + 3k_x^2 k_y^4 \right) a^{-4}(\mathbf{k}_0) \right\} |u|^4 \right] dY dX.$$

Their expressions in the two-dimensional case follow directly, namely

$$iu_\tau = \frac{1}{\varepsilon^2} \left(\omega(k_0 + \varepsilon D_X) - \omega(k_0) \right) u - \left(\frac{k_0^4 a^{-2}(2k_0) a^4(k_0)}{4\omega(2k_0)} - \frac{1}{2} k_0^3 + \frac{5\mathcal{D}}{4\rho} k_0^6 a^{-4}(k_0) \right) |u|^2 u,$$

and

$$H = \int_{-\infty}^{\infty} \left[\frac{1}{\varepsilon^2} \bar{u} \left(\omega(k_0 + \varepsilon D_X) - \omega(k_0) \right) u - \left(\frac{k_0^4 a^{-2}(2k_0) a^4(k_0)}{8\omega(2k_0)} - \frac{1}{4} k_0^3 + \frac{5\mathcal{D}}{8\rho} k_0^6 a^{-4}(k_0) \right) |u|^4 \right] dX.$$

4 Conclusions

A Hamiltonian formulation for three-dimensional nonlinear flexural-gravity waves propagating at the surface of an ideal fluid covered by ice is presented. The ice sheet is modeled as a thin elastic plate, based on the special Cosserat theory for hyperelastic shells as proposed by Plotnikov and Toland [34]. Weakly nonlinear models for small-amplitude waves on finite and infinite depth are derived in the modulational regime, by applying the Hamiltonian perturbation approach of

Craig et al. [8, 10]. A new contribution of the present paper is the inclusion of second-harmonic effects, leading to corrections in the cubic coefficient of the envelope equations and in the expression of the ice-sheet deflection. However, comparison with two-dimensional direct numerical simulations reveals no much improvement from these higher-order corrections in the parameter regime considered.

In the future, it would be of interest to further analyze the resulting NLS and DS equations, in particular those incorporating exact linear dispersion, and to compute localized traveling solutions numerically. We also plan to investigate the long-wave regime for this three-dimensional hydroelastic problem within the Hamiltonian framework.

Acknowledgements This work was partially supported by the Simons Foundation through grant No. 246170. The author thanks Walter Craig, Emilian Părău and Catherine Sulem for fruitful discussions. Part of this work was carried out while the author was visiting the Isaac Newton Institute for Mathematical Sciences during the Theory of Water Waves program in the summer 2014.

References

1. Ablowitz, M.J., Segur, H.: Evolution of packets of water waves. *J. Fluid Mech.* **92**, 691–715 (1979)
2. Akylas, T.R.: Envelope solitons with stationary crests. *Phys. Fluids* **5**, 789–791 (1993)
3. Alam, M.R.: Dromions of flexural-gravity waves. *J. Fluid Mech.* **719**, 1–13 (2013)
4. Bonnefoy, F., Meylan, M.H., Ferrant, P.: Nonlinear higher-order spectral solution for a two-dimensional moving load on ice. *J. Fluid Mech.* **621**, 215–242 (2009)
5. Craig, W., Guyenne, P., Kalisch, H.: Hamiltonian long wave expansions for free surfaces and interfaces. *Commun. Pure Appl. Math.* **58**, 1587–1641 (2005)
6. Craig, W., Guyenne, P., Nicholls, D.P., Sulem, C.: Hamiltonian long-wave expansions for water waves over a rough bottom. *Proc. R. Soc. A* **461**, 839–873 (2005)
7. Craig, W., Guyenne, P., Sulem, C.: Water waves over a random bottom. *J. Fluid Mech.* **640**, 79–107 (2009)
8. Craig, W., Guyenne, P., Sulem, C.: A Hamiltonian approach to nonlinear modulation of surface water waves. *Wave Motion* **47**, 552–563 (2010)
9. Craig, W., Guyenne, P., Sulem, C.: Coupling between internal and surface waves. *Nat. Hazards* **57**, 617–642 (2011)
10. Craig, W., Guyenne, P., Sulem, C.: Hamiltonian higher-order nonlinear Schrödinger equations for broader-banded waves on deep water. *Eur. J. Mech. B. Fluids* **32**, 22–31 (2012)
11. Craig, W., Guyenne, P., Sulem, C.: The surface signature of internal waves. *J. Fluid Mech.* **710**, 277–303 (2012)
12. Craig, W., Guyenne, P., Sulem, C.: Internal waves coupled to surface gravity waves in three dimensions. *Commun. Math. Sci.* **13**, 893–910 (2015)
13. Craig, W., Schanz, U., Sulem, C.: The modulational regime of three-dimensional water waves and the Davey–Stewartson system. *Ann. Inst. H. Poincaré (C) Nonlinear Anal.* **14**, 615–667 (1997)
14. Craig, W., Sulem, C.: Numerical simulation of gravity waves. *J. Comput. Phys.* **108**, 73–83 (1993)

15. Craig, W., Sulem, C., Sulem, P.-L.: Nonlinear modulation of gravity waves: a rigorous approach. *Nonlinearity* **5**, 497–522 (1992)
16. Düll, W.-P., Schneider, G., Wayne, C.E.: Justification of the Nonlinear Schrödinger equation for the evolution of gravity driven 2D surface water waves in a canal of finite depth. (2013, submitted)
17. Forbes, L.K.: Surface waves of large amplitude beneath an elastic sheet. Part 1. High-order series solution. *J. Fluid Mech.* **169**, 409–428 (1986)
18. Grillakis, M., Shatah, J., Strauss, W.: Stability theory of solitary waves in the presence of symmetry. *I. J. Funct. Anal.* **74**, 160–197 (1987)
19. Guyenne, P., Lannes, D., Saut, J.-C.: Well-posedness of the Cauchy problem for models of large amplitude internal waves. *Nonlinearity* **23**, 237–275 (2010)
20. Guyenne, P., Nicholls, D.P.: A high-order spectral method for nonlinear water waves over moving bottom topography. *SIAM J. Sci. Comput.* **30**, 81–101 (2007)
21. Guyenne, P., Părău, E.I.: Computations of fully nonlinear hydroelastic solitary waves on deep water. *J. Fluid Mech.* **713**, 307–329 (2012)
22. Guyenne, P., Părău, E.I.: Forced and unforced flexural-gravity solitary waves. In: *Proceedings of IUTAM Nonlinear Interfacial Wave Phenomena from the Micro- to the Macro-Scale*, vol. 11, pp. 44–57. Limassol (2014)
23. Guyenne, P., Părău, E.I.: Finite-depth effects on solitary waves in a floating ice sheet. *J. Fluids Struct.* **49**, 242–262 (2014)
24. Hărăguș-Courcelle, M., Ilichev, A.: Three-dimensional solitary waves in the presence of additional surface effects. *Eur. J. Mech. B. Fluids* **17**, 739–768 (1998)
25. Hegarty, G.M., Squire, V.A.: A boundary-integral method for the interaction of large-amplitude ocean waves with a compliant floating raft such as a sea-ice floe. *J. Eng. Math.* **62**, 355–372 (2008)
26. Korobkin, A., Părău, E.I., Vanden-Broeck, J.-M.: The mathematical challenges and modelling of hydroelasticity. *Philos. Trans. R. Soc. Lond. A* **369**, 2803–2812 (2011)
27. Lannes, D.: *The Water Waves Problem: Mathematical Analysis and Asymptotics*. American Mathematical Society, Providence (2013)
28. Marko, J.R.: Observations and analyses of an intense waves-in-ice event in the Sea of Okhotsk. *J. Geophys. Res.* **108**, 3296 (2003)
29. Milewski, P.A., Vanden-Broeck, J.-M., Wang, Z.: Hydroelastic solitary waves in deep water. *J. Fluid Mech.* **679**, 628–640 (2011)
30. Milewski, P.A., Wang, Z.: Three dimensional flexural-gravity waves. *Stud. Appl. Math.* **131**, 135–148 (2013)
31. Nicholls, D.P.: Traveling water waves: Spectral continuation methods with parallel implementation. *J. Comput. Phys.* **143**, 224–240 (1998)
32. Părău, E., Dias, F.: Nonlinear effects in the response of a floating ice plate to a moving load. *J. Fluid Mech.* **460**, 281–305 (2002)
33. Părău, E.I., Vanden-Broeck, J.-M.: Three-dimensional waves beneath an ice sheet due to a steadily moving pressure. *Phil. Trans. Roy. Soc. Lond. A* **369**, 2973–2988 (2011)
34. Plotnikov, P.I., Toland, J.F.: Modelling nonlinear hydroelastic waves. *Philos. Trans. R. Soc. Lond. A* **369**, 2942–2956 (2011)
35. Schneider, G., Wayne, C.E.: Justification of the NLS approximation for a quasilinear water wave model. *J. Differ. Equ.* **251**, 238–269 (2011)
36. Squire, V.A.: Past, present and impendent hydroelastic challenges in the polar and subpolar seas. *Philos. Trans. R. Soc. A* **369**, 2813–2831 (2011)
37. Squire, V.A., Hosking, R.J., Kerr, A.D., Langhorne, P.J.: *Moving Loads on Ice Plates*. Kluwer, Dordrecht (1996)
38. Sulem, C., Sulem, P.-L.: *The Nonlinear Schrödinger Equation: Self-focusing and Wave Collapse*. Springer, New York (1999)
39. Takizawa, T.: Deflection of a floating sea ice sheet induced by a moving load. *Cold Reg. Sci. Technol.* **11**, 171–180 (1985)

40. Totz, N., Wu, S.: A rigorous justification of the modulation approximation to the 2D full water wave problem. *Commun. Math. Phys.* **310**, 817–883 (2012)
41. Trulsen, K., Kliakhandler, I., Dysthe, K.B., Velarde, M.G.: On weakly nonlinear modulation of waves on deep water. *Phys. Fluids* **12**, 2432–2437 (2000)
42. Vanden-Broeck, J.-M., Pärä, E.I.: Two-dimensional generalised solitary waves and periodic waves under an ice sheet. *Philos. Trans. R. Soc. Lond. A* **369**, 2957–2972 (2011)
43. Xia, X., Shen, H.T.: Nonlinear interaction of ice cover with shallow water waves in channels. *J. Fluid Mech.* **467**, 259–268 (2002)
44. Xu, L., Guyenne, P.: Numerical simulation of three-dimensional nonlinear water waves. *J. Comput. Phys.* **228**, 8446–8466 (2009)
45. Zakharov, V.E.: Stability of periodic waves of finite amplitude on the surface of a deep fluid. *J. Appl. Mech. Tech. Phys.* **9**, 190–194 (1968)